A New Framework for Evaluating Model Simulated Inland Tropical Cyclone Wind Fields

Jie Chen[1], Kun Gao[1], Lucas Harris[2], Timothy Marchok[2], Linjiong Zhou [1], Matthew Morin[2]

[1]The Program in Atmospheric and Oceanic Sciences, Princeton University, Princeton, NJ
[2]NOAA Geophysical Fluid Dynamics Laboratory (GFDL), Princeton, NJ

Key Points:

- We introduce a new framework for evaluating modeled inland tropical cyclone wind fields with observation-based, theory-driven wind profiles.
- The theory-driven wind profile well represents the observed radial distribution of inland tropical cyclone wind speeds.
- We propose simple indicators to summarize the model performance on inland wind field predictions.

Corresponding author: Jie Chen, `chenjie@princeton.edu`

Abstract

Though tropical cyclone (TC) models have been routinely evaluated against track and intensity observations, little work has been performed to validate modeled TC wind fields over land. In this paper, we present a simple framework for evaluating simulated low-level inland winds with in-situ observations and existing TC structure theory. The Automated Surface Observing Systems, Florida Coastal Monitoring Program, and best track data are used to generate a theory-driven wind profile that reasonably represents the observed radial distribution of TC wind speeds. We quantitatively and qualitatively evaluated the modeled inland TC wind fields, and described the model performance with a set of simple indicators. The framework was used to examine the performance of a high-resolution two-way nested Geophysical Fluid Dynamics Laboratory model on recent U.S. landfalling TCs. Results demonstrate the capacity of using this framework to assess the modeled TC low-level wind field in the absence of dense inland observations.

Plain Language Summary

Some of the biggest human impacts of tropical cyclone (TC) winds come after the TC makes landfall. A skillful prediction of the radial distribution of winds is essential for forecasting TC-induced inland hazards. However, the forecast skill of numerical hurricane models on inland TC wind fields has rarely been evaluated since it is challenging to collect wind observations during landfall, and the network of regular weather observations is too spread out to capture the strongest winds associated with a TC. This inhibits the improvement of forecast models and limits our understanding of the TC's inland evolution. Our work combines available inland in-situ wind observations over the southeastern U.S. with existing TC structure theory, and presents a new "optimal" estimate of the post-landfall winds. Our framework is found to be useful for evaluating the post-landfall TC winds in hurricane forecast models. In addition, the new evaluation technique can intuitively demonstrate how well the model simulates TC intensity and structure.

1 Introduction

Landfalling tropical cyclones (TCs) bring significant hazards and cause enormous economic losses (Villarini et al., 2014; Rappaport, 2014). These impacts could be amplified in a changing climate, given the potential that landfalling TCs may move and decay more slowly in a warming climate (Kossin, 2018, 2019; Li & Chakraborty, 2020; Chan et al., 2022), and compound hazards may increases under climate change (Gori & Lin, 2022; Feng et al., 2022). Beyond that, research suggests that TCs may make landfall in unusual regions that are more vulnerable to TC hazards due to a shift in landfall location and to a possible poleward shift in the latitude of maximum intensity in a warmer future climate (Kossin et al., 2014; Knutson & Coauthors, 2020). Indeed, even without the effects of climate change, TC damage is likely to double in the future since there are more people and assets in harm's way (Mendelsohn et al., 2012). Therefore, it is urgent to evaluate the post-landfall performance of hurricane models, especially for predicting the low-level TC wind field, since inland hazards and weather extremes are intimately linked to the wind field structure (Zhai & Jiang, 2014).

Though in-situ observations are essential for evaluating the simulation of inland TC low-level wind fields (Nolan et al., 2021), our community lacks dense and systematic observations of the TC low-level wind field after landfall. As such, it is necessary to introduce alternative analyses for the evaluation of modeled inland TC winds. In this work, we form a framework assessing the model performance on predicting inland TC wind fields using observation-based, theory-driven wind profiles. This wind profile is generated from existing TC structure models given observable TC parameters obtained primarily from the available observations. Beyond the widely-used International Best Track Archive for Climate Stewardship (IBTrACS version 4, Knapp et al. (2010)) for TC intensity and track, the

minute-by-minute, near-surface observations provided by the Automated Surface Weather Observations (ASOS) and the Florida Coastal Monitoring Program (FCMP) are also used. The model evaluated in this work is the Tropical Atlantic version of Geophysical Fluid Dynamics Laboratory (GFDL)'s System for High-resolution prediction on Earth-to-Local Domains (T-SHiELD hereafter), which will be introduced in the following section. T-SHiELD has shown skillful predictions of TC landfall track and intensity (Harris et al., 2020; Gao et al., 2021). Since T-SHiELD shares much of the code with the NOAA's next-generation Hurricane Analysis and Forecast System (HAFS) and also includes advanced features developed at GFDL for better hurricane predictions, it serves as a good representative model for the evaluation. Moreover, this work attempts to quantify the performance of the model on simulated wind fields via a set of time-dependent indicators that describe the characteristics of the forecast error. These evaluations can reveal the performance of model predictions for landfalling cases and quantify the improvement of forecast skills associated with the model development.

In this paper, we first introduce the datasets, the GFDL T-SHiELD model, and the assessment framework (Section 2). Then we analyze the performance of the simulated T-SHiELD inland wind fields via the evaluation framework and the performance indicators (Section 3). We end with a summary and discussion (Section 4).

2 Data and Methods

2.1 Observation and model data

We use TC track and intensity data from IBTrACS version 4 for selected 2020–2022 landfalling storms in the contiguous United States. Recent studies suggest that the data accuracy has been improved through years with advanced technology (Landsea, 2007; Landsea & Franklin, 2013; Zhu & Collins, 2021). Therefore, this work considers the IBTrACS reports as a baseline reference for the inland TC track and intensity change. The representative landfalling cases are the storms during the 2020-2022 hurricane seasons to strike along the coastlines of the Gulf of Mexico and the Florida peninsula: Laura (2020), Sally (2020), Delta (2020), Fred (2021), Ida (2021), and Ian (2022) (Figure 1). Except for Fred, which represents a low-intensity landfalling TC, selection of landfall cases is defined following the criteria used in Zhu and Collins (2021), but with a few modifications, including that the TC intensity upon first U.S. inland point must be Category 1 or higher (maximum wind speed ≥ 64 kts), and the intensity remains higher than 34 kts for at least 12 hours before dissipation or extratropical transition. This criteria enables a close and sufficiently lengthy examination after landfall while excluding the influences on TC intensity and structure from extratropical transition at higher latitudes (Evans & Hart, 2003).

We use several in-situ datasets for wind observations in addition to the IBTrACS: 1) ASOS wind data at each 5-min interval across 11 southeastern states obtained from the National Centers for Environmental Information (NCEI) and processed by Iowa Environmental Mesonet at Iowa State University (Figure 2a). Due to the destructive power of TC winds, ASOS sites near the eyewall may be missing validated wind records during the landfall. 2) the FCMP mobile tower observations (Masters et al., 2010; Balderrama et al., 2011). The FCMP 10-m mobile towers, T1 (29.44N,90.26W) and T5 (29.76N,90.56W) (Figure 1) are deployed to record Hurricane Ida's wind speed every 0.1s, which are applied for additional analyses (Supplementary Figure 5).

The dynamical model to be evaluated is the GFDL T-SHiELD that is initialized by six-hourly National Centers for Environmental Prediction (NCEP) Global Forecast System (GFS) analyses, which is used to provide near real-time forecasts during recent hurricane season (Harris et al., 2020; Gao et al., 2021). The model applies the non-hydrostatic Finite-Volume Cubed-Sphere Dynamical Core (FV3) with a 3-km-resolution nested domain covering the southeast U.S. and western Atlantic and 75 vertical levels (Chen et al., 2019; Zhou
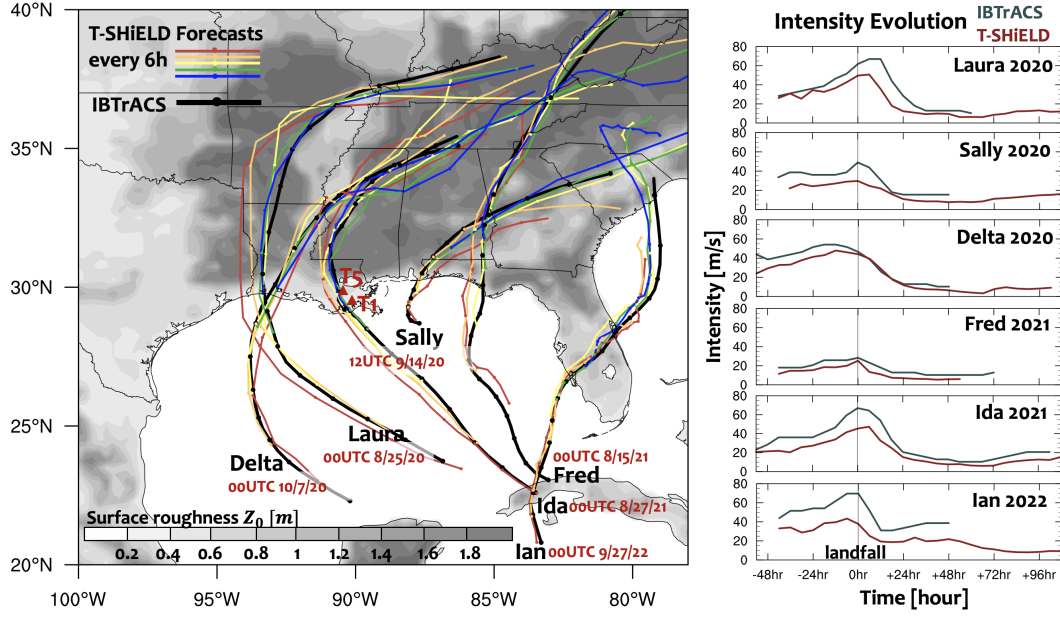
Figure 1. T-SHiELD tracks of six selected 2020-2022 U.S. landfalling hurricanes, initialized every six hours starting from the labeled time (colored tracks), and the corresponding IBTrACS tracks (thick black track). The evolution of the predicted mean intensity averaged over the successive T-SHiELD forecasts (red) is compared to the IBTrACS intensity (black) in the right panel. The evolution time shown in the X-axis is referenced by each landfall time reported by the IBTrACS. The two FCMP mobile towers T1 (29.44N,90.26W) and T5 (29.76N,90.56W) for Hurricane Ida (2021) are marked on the map with red triangles. The surface roughness (Z_0) obtained from the Fifth generation of ECMWF atmospheric reanalyses of the global climate (ERA5) will be used to calculate the surface drag coefficient in this work (see Appendix A).

et al., 2019; Gao et al., 2021; Harris et al., 2021). For representative cases in this work, forecasts initialized from different times before landfall show consistent intensity and track prediction. To avoid a weakening of the wind field characteristics when using the mean wind field averaged over the successive T-SHiELD forecasts (Figure 1 left), we pick the T-SHiELD forecast initialized 12 hours prior to the observed landfall time for each case. That is, the T-SHiELD forecast time since the landfall is 12 hours plus the observation time in this work. We produce model output every 15 minutes for comparison to high-frequency ASOS data.

2.2 The evaluation framework

2.2.1 Wind speed radial distribution

ASOS sites are unevenly distributed and sparse. To alleviate this problem, we produce radial wind speed distributions from ASOS sites in each TC quadrant. The four earth-relative quadrants are identified by the observed, time-dependent TC center (Figure 2a-b, blue). Given that IBTrACS provides TC location every 3 or 6 hours, the ASOS radial wind distribution is also generated every 3 or 6 hours. Correspondingly, the nearest T-SHiELD grid points to each ASOS site are selected and formed into the radial wind speed distributions based on simulated TC locations at each observed time (Figure 2a-b, red). Adjacent ASOS sites may have the same corresponding T-SHiELD grid point due to the site sparsity in some areas. For a more consistent comparison, the maximum wind speed recorded by each ASOS site during the analyzed observation hour will be selected from its

twelve records at each 5-minute interval to represent the hourly wind speed, and similarly, the T-SHiELD modeled wind speed maxima during the same hourly period are selected from the outputs.

2.2.2 *The observation-based, theory-driven wind profile*

In addition to the direct site-by-site wind comparison between ASOS and T-SHiELD as shown in Fig.2b, we introduce an observation-based, theory-driven inland TC wind profile for further quantitative assessments. The Chavas et al. (2015) wind field model (referred to as C15 hereafter) is a simple theoretical model formed by mathematically merging the Emanuel and Rotunno (2011) inner wind field model and Emanuel (2004) outer wind field model. With a small number of physical parameters, C15 captures the structure of the observed TC wind field over the ocean, and has been applied in TC surge risk simulations and analysis (Xi et al., 2020; Lin et al., 2020; Wang et al., 2022). For post-landfall TC evolution, the C15 model well-reproduces the simulated wind field in response to idealized landfalls (Chen & Chavas, 2023). Using the observed parameters to generate a theoretical post-landfall wind field is a natural attempt to link the theoretical understanding to the real-world applications. The full solutions of using the C15, including how environmental approximations are calculated are provided in the Appendix A. Essential parameters required to generate the radial wind profile are the TC intensity (v_m) and any wind radius (e.g., radius of 10 ms^{-1} wind, referred to as r_{10} hereafter).

Here we use our observed wind profiles to generate the required input parameters for the C15 wind profile. Given the ASOS wind speed radial distribution, we first fit a cubic spline to identify the representative $r_{10}(\tau)$, or $r_5(\tau)$ when $r_{10}(\tau)$ is not applicable, for the wind field in each quadrant (Figure 2c, dash line), where τ is the time since TC landfall. For the TC intensity after landfall, $v_m(\tau)$, which is not reliably captured by the ASOS or FCMP, we use the widely-applied sustained maximum wind speed from IBTrACS. We call this theoretical inland TC wind profile in each quadrant the *observation-based, theory-driven wind profile* (Obs-Theo hereafter). For further quantitative assessment, the Obs-Theo wind profile will be used to verify the T-SHiELD wind profile as in Figure 2d, as long as the required parameters are available from the observational datasets. In the quantitative evaluation, the T-SHiELD wind profile is azimuthally-averaged based on all model grid points in each quadrant, and smoothed by averaging over every several points along each selected arc to reduce noise from various maxima and minima in the wind data, which is necessary for a high-resolution model.

Notably, with just size parameters from the cubic spline fit, the Obs-Theo wind profile well represents the observed wind speed distribution in the outer region ($r = 200 - 600\ km$) with a small root-mean-square error (2-3 ms^{-1}) that slightly increases with the forecast time in selected landfall case (Supplementary Figure 1). For the inner region, where we lack a dense network of ASOS observations, the Obs-Theo profile is primarily determined by the IBTrACS v_m. As shown in Supplementary Figure 2a, at 1800UTC 29 Aug 2021, the Obs-Theo inner wind profile can vary remarkably given IBTrACS v_m or FCMP-recorded v_m that differ significantly (Supplementary Figure 2b). In the absence of dense observations, it is challenging to verify the Obs-Theo inner wind profile. FCMP along the landfall track is not routinely provided for every landfall TC. Future work could explore using an alternative v_m other than that from IBTrACS, or testing the Obs-Theo profile against specific cases with dense inner region observations.
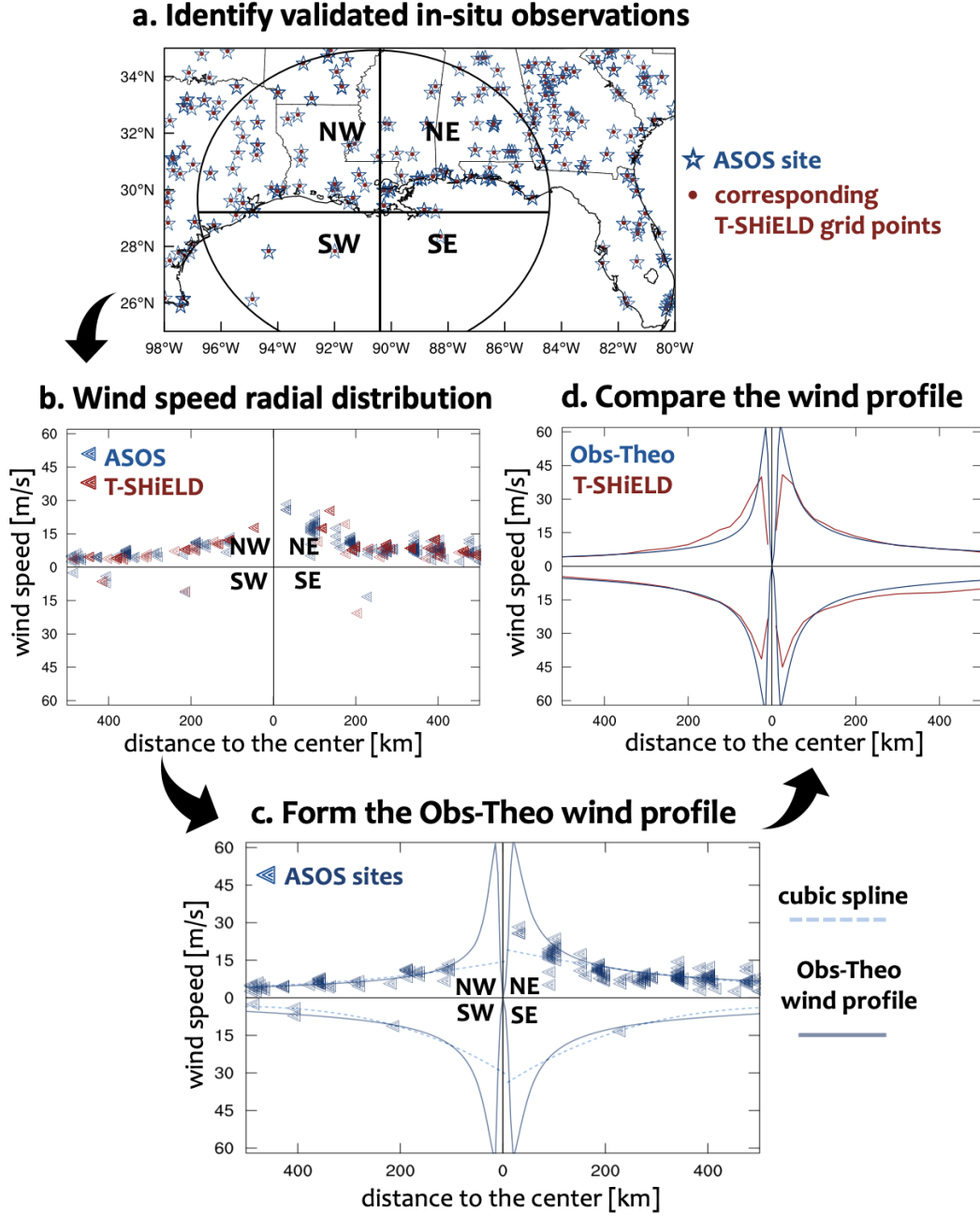
Figure 2. Schematic for the evaluation framework using Hurricane Ida at 1800UTC 29 Aug 2021 as an example. (a) The locations of the validated ASOS sites and their corresponding nearest T-SHiELD grid points. The analyzed area ($r \leq 600\ km$) from the observed TC center is divided into four earth-relative quadrants. (b) In each quadrant of (a), the hourly-maximum wind speed values of all the ASOS sites and T-SHiELD grid points are lined into a wind speed radial distribution based on their distance to the observed or simulated TC center, respectively. (c) The observation-based, theory-driven (Obs-Theo) wind profile (solid curve) for Ida at this time, where the maximum wind speed v_m is obtained from IBTrACS, the representative radius r_{10} for the wind field in each quadrant is obtained from the cubic spline (dash curve) of the ASOS wind speed radial distribution. The average root-mean-square deviation of ASOS observations from the Obs-Theo wind profile is $2\ ms^{-1}$. (d) A comparison of the Obs-Theo and the T-SHiELD wind profiles in each quadrant at this time for Ida. The T-SHiELD wind profile is generated based on all model grid points in each quadrant.

3 Assessing the T-SHiELD performance on inland TC wind field

Hurricane Ida (2021), a destructive Category 4 hurricane, is the second most-damaging hurricane to hit Louisiana in history (Beven et al., 2021). The post-landfall remnants of Ida also caused catastrophic damages from flooding and thunderstorms across the Northeastern states (Smith et al., 2023). Here we use Ida as an example to show the evaluation framework.

The direct comparison of the Ida inland wind speed radial distributions between ASOS observations and T-SHiELD forecast, similar to Figure 2b, are provided in the supplementary materials, along with the results of other representative cases (Supplementary Figure 3-5). Overall, the T-SHiELD forecast reproduces the observed post-landfall structural change of the wind speed radial distribution. However, the direct comparison of the wind speed radial distribution cannot quantitatively show the performance of the T-SHiELD forecast, especially when ASOS lacks validated data near the eyewall or over the ocean. Therefore, we evaluate the T-SHiELD wind profile with the Obs-Theo wind profile for further quantitative assessments as introduced in Figure 2c-d.

3.1 Wind profile comparison: using model performance indicators

To ensure a uniform comparison across cases with varying storm structures and sizes, characteristic wind profiles, $\tilde{v}(\tilde{r})$, are used here (Chavas & Knaff, 2022; Klotzbach et al., 2022), where the wind speed is normalized by the observed maximum wind speed v_m from IBTrACS as $\tilde{v} = v/v_m$, and radius is normalized by the radius of maximum wind speed r_m identified by the Obs-Theo wind profile as $\tilde{r} = r/r_m$. We only assess the wind field outside r_m ($\tilde{r} > 1$) since neither the theory nor the forecast model can well describe or simulate the wind field inside r_m. We divide the wind field into inner region ($1 < \tilde{r} < 3$) and outer region ($\tilde{r} > 3$) for more in-depth analysis.

Using Hurricane Ida at 1800UTC 29 Aug 2021 as an example, the characteristic wind profiles of Obs-Theo and T-SHiELD are compared in each quadrant, respectively (Figure 3). The wind speed difference $\triangle\tilde{v}$ between the T-SHiELD forecast and Obs-Theo along the characteristic radius $\tilde{r}$ is defined as the error profile, $\triangle\tilde{v}(\tilde{r})$. In this way, the shape of the error profile explains the performance of T-SHiELD on the inland wind field simulation. We use a simple linear fit to the error profile in each region, as

$$\triangle\tilde{v} = \left\{ \begin{array}{ll} \beta(\tilde{r}-1) + \alpha, & 1 < \tilde{r} < 3 \\ \beta(\tilde{r}-3) + \alpha, & \tilde{r} > 3 \end{array} \right. \tag{1}$$

where the two indicators, α and β together describe characteristics of the error profile —the performance of the T-SHiELD wind field forecast—at a single time for a selected storm.

We name α, the y-intercept, as the wind field *bias indicator*, the value of which reflects the normalized T-SHiELD forecast bias at $\tilde{r} = 1$ or 3. Negative α indicates a weaker wind field forecast at the starting point of inner or outer wind region. β, the slope of $\triangle\tilde{v}(\tilde{r})$, describes how the forecast error changes along the radius from the starting point of each region, and is defined as the wind profile *shape indicator*. For both α and β, lower magnitudes suggest better wind field simulations, as $(\alpha, \beta = 0)$ indicates the modeled wind profile exactly matching the observed one. In this work, "best forecast" is defined by both indicators that have a magnitude smaller than $O(10^{-2})$. For example, the near-zero α and β in the outer regions suggest a T-SHiELD simulation comparable to the corresponding Obs-Theo wind profiles in the NE, SE, and NW quadrants (Figure 3a, b and d, purple fit curves). However, in the SW quadrant, the higher magnitude of α ($\sim -10^{-1}$) and the near-zero β indicates a uniform weaker wind field simulation among the outer region (Figure 3c). In contrast to the well-simulated outer region, T-SHiELD shows a weaker forecast bias gradually increasing towards the r_m within the inner region (Figure 3, yellow fit curve). In this Ida example, the IBTrACS $v_m = 64.3\ ms^{-1}$ at 1800UTC, thus the value of inner-region α can be translated into a weaker intensity bias up to tens of ms^{-1} at $\tilde{r} = 1$. More examples interpreting the values of α and β are shown in Supplementary Figure 6.
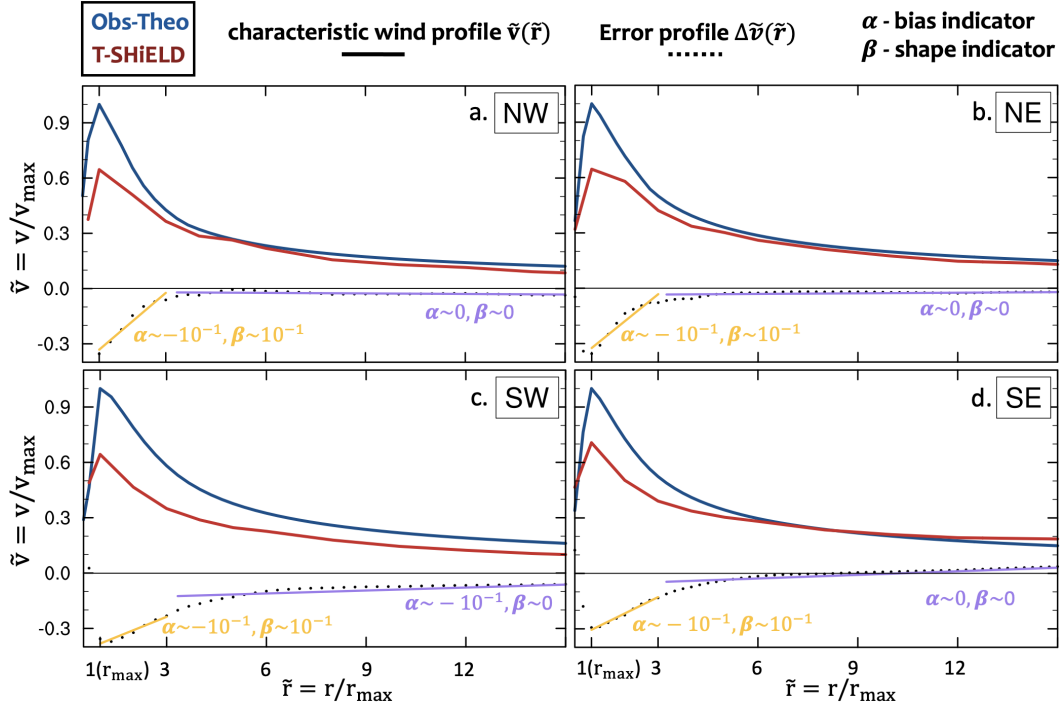
Figure 3. The comparison of characteristic wind profile $\tilde{v}(\tilde{r})$ between the Obs-Theo profile (blue line) and the T-SHiELD wind profile (red line) for Hurricane Ida at 1800UTC 29 Aug 2021. The error profile $\triangle\tilde{v}(\tilde{r})$ (dash curve) is linearly fitted among the inner region (yellow line, $1 < \tilde{r} < 3$) and outer region (purple line, $\tilde{r} > 3$), respectively. α is defined as the wind field bias and β is defined as the wind profile shape indicator. $v_m = 64.3\ ms^{-1}$ is obtained from the IBTrACS.

3.2 Composite results of 2020-2022 selected Hurricanes

Given the value of averaged $\alpha(\tau)$ and $\beta(\tau)$ in each quadrant of all representative TCs, where τ indicates the time since the observed landfall, we can examine the overall performance of T-SHiELD simulated inland wind field for the 2020-2022 selected hurricanes.

For inner regions, α and β do not fall in the "best forecast" interval (Figure 4a-d, grey shaded area). The values of α and β indicate that T-SHiELD underestimates the maximum wind speed v_m, leading to a weaker wind field forecast where the forecast error increases towards the r_m (Similar to Figure 3a). There is no clear trend for $\alpha(\tau)$ and $\beta(\tau)$ in each quadrant after landfall, suggesting that the T-SHiELD performance on the inner wind field does not change significantly after landfall. However, for the outer region, T-SHiELD wind profiles are comparable to the Obs-Theo in each quadrant (Figure 4e-h). Despite the NW quadrant (Figure 4e), both α and β largely fall in the "best forecast" interval after the landfall, indicating a -forecast outer wind field across different cases.

To summarize, the value of indicators $\alpha(\tau)$ and $\beta(\tau)$ suggests that T-SHiELD mostly struggles with representing the inner-core wind structure of landfalling TCs. The relatively large negative $\alpha(\tau)$ values (Fig. 4a-d) suggest the structural biases are related to the negative model intensity biases (Figure 1). Therefore, improving the T-SHIELD intensity forecasts, for example, through a vortex-specific initialization technique, may significantly improve its performance on the overall wind field forecast.
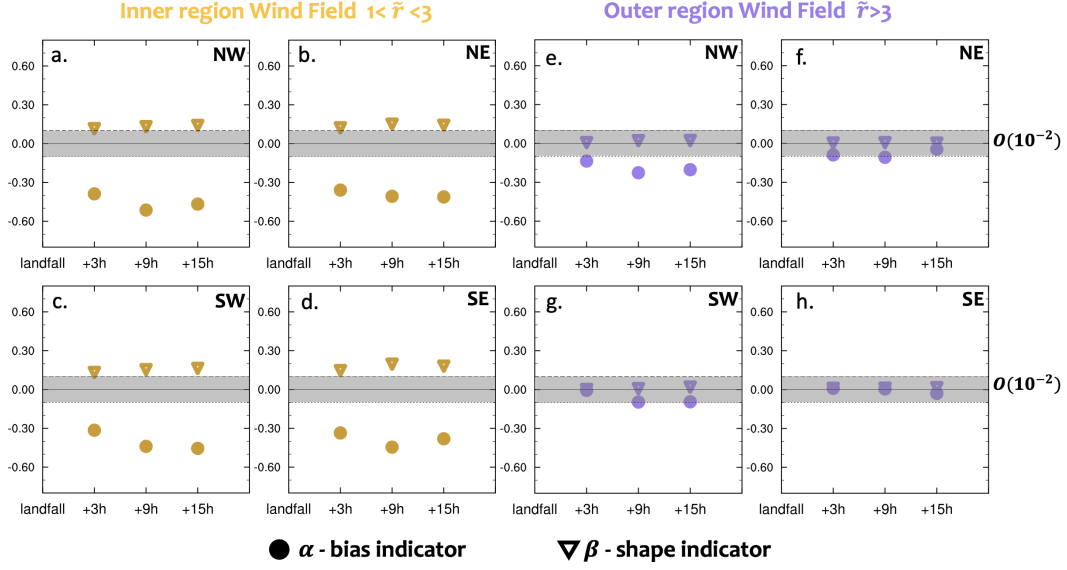
Inner region Wind Field $1 < \tilde{r} < 3$ **Outer region Wind Field** $\tilde{r} > 3$

Figure 4. The averaged $\alpha(\tau)$ and $\beta(\tau)$ of six 2020-2022 major hurricanes at discrete lead times after their corresponding landfalls, which describe the T-SHiELD performance on predicting the inland low-level wind field. Left panels show the inner region wind field ($1 < \tilde{r} < 3$), and right panels for the outer wind field ($\tilde{r} > 3$). α indicates the normalized intensity bias of the T-SHiELD forecasts compared to the observations at $\tilde{r} = 1$ or 3, while β indicates the shape similarity between the observed and T-SHiELD wind profiles. The indicator magnitudes ranging from -0.1 to 0.1 are shaded, where 0 indicates a perfect simulation (no forecast error). Indicators falling in the shaded interval suggest a "best forecast" in this work.

4 Summary

This work presents a novel framework for assessing the model performance on predicting the inland TC low-level wind using the observation-based, theory-driven wind profile that combines the ASOS observations and the existing theoretical TC wind field model. Although the evaluation in this paper only focuses on the performance of the GFDL T-SHiELD on six major landfalling hurricanes in the continental U.S. along the Gulf of Mexico coast from 2020 to 2022, the evaluation framework can be generalized to other model evaluations emphasizing the TC wind field.

In our framework, we introduce several observation-based evaluation approaches into the wind field assessment. The ASOS wind speed radial distribution, which generally depicts the TC asymmetric structural change shortly after landfall, can directly be used to qualitatively evaluate the model overall forecast of the inland TC wind field. Then, the wind profile in each quadrant generated by the theoretical wind field model given observable TC parameters (r_{10}, v_m) obtained from ASOS and IBTrACS enables further quantitative evaluations for the simulated inland wind field. This Obs-Theo wind profile well represents the observed wind speed distribution in the outer region. Finally, the forecast error along the radius (i.e., error profile) is linearly fitted among the inner and outer regions, described by the wind field bias indicator and wind profile shape indicator of the fitted lines. These indicators quantitatively reveal the performance of the model on inland TCs, and can also be used in future work to reveal the improvement in wind field forecast skill associated with the model development.

Compared to TC track and intensity, the post-landfall evolution of the TC low-level wind field has not received much attention in previous model evaluation studies due to the complexity of the TC structural change and the lack of in-situ inland wind field observations. This wind field evaluation framework provides an alternative approach assessing the model directly with in-situ observations taking advantage of existing TC structure theory. However, our community still needs to advance the post-landfall TC observations, especially among the eyewall region, and provide reliable routinely-used TC datasets to strengthen our studies on inland TC hazards and their evolution.

5 Open Research

The GFDL T-SHiELD outputs, processed ASOS data, and the observation-based, theory-driven wind profile data used in this work are available on Zenedo (DOI 10.5281/zenodo.7937697). The IBTrACS data is available at `https://climatedataguide.ucar.edu/climate-data/ibtracs-tropical-cyclone-best-track-data`. The ASOS data applied in this work is available at Iowa State University (`https://mesonet.agron.iastate.edu/ASOS/`). The FCMP data of hurricane Ida is is available by contacting Prof. David Nolan at University of Miami. The C15 wind structure model is available at `https://doi.org/doi:10.4231/CZ4P-D448`.

Appendix A C15 wind field model

The C15 model mathematically merged the Emanuel and Rotunno (2011) inner wind field model (Eq.36 therein) and Emanuel (2004) outer wind field model (Eq.31-33 therein) solution to produce a model for the complete azimuthal wind profile. This merging yields a unique solution; the process is described in C15 (Eq.2-10 therein). Using C15, parameters required to solve the differential equations for the wind profile are: storm intensity v_m, radius of maximum wind speed r_m for the inner region, the intensity and radius of the merge point connecting the inner and outer region, v_a and r_a, and a specified radius input r_{fit}, χ and Coriolis parameter f for the environmental conditions where $\chi = \frac{2C_d}{W_{cool}}$. C_d is the exchange coefficients of momentum, W_{cool} is the free tropospheric subsidence rate. The value of W_{cool} is constrained by the thermodynamics of the free troposphere and can be estimated from the ambient stratification and radiative cooling rate via radiative-subsidence balance. Given the environmental parameters χ and f, one only needs to know two storm parameters – the intensity v_m and any wind radius (e.g. r_m, r_{17}, or r_{10}) – to specify the model solution.

In this work, v_m and r_{10} are primarily obtained from IBTrACS and ASOS observations. f is calculated by the TC location provided by IBTrACS; C_d is calculated from the Fifth generation of ECMWF atmospheric reanalyses of the global climate (ERA5) surface roughness (Hersbach, 2010) and then averaged within $r = 0-600\ km$ to yield a single value within each of the four earth-relative quadrants (Figure 1). Previous work testing C15 against idealized landfall suggests that, the wind field solution is not very sensitive to W_{cool} except for at large radii. Thus, the radiative-subsidence rate W_{cool} is set to 0.002 ms^{-1}, which is the median of the best-fit value for observed storms (Chavas et al., 2015) and identical to idealized experiments in Chen and Chavas (2023) and related studies.

References

Balderrama, J., Masters, F., Gurley, K., Prevatt, D., Aponte-Bermudez, L., Reinhold, T., . . . Chowdhury, A. (2011). The Florida Coastal Monitoring Program (FCMP): A review. *Journal of Wind Engineering and Industrial Aerodynamics*, *99(9)*, 979-995.

Beven, J. L., Hagen, A., & Berg, R. (2021). *Hurricane Ida (AL092021).* (Tropical Cyclone Report). National Hurricane Center. (Available from National Hurricane Center)

Chan, K., Zhang, K., Wu, Y., & Chan, J. C. L. (2022). Landfalling Hurricane Track Modes and Decay. *Nature*, *606*, E7-E11.

Chavas, D. R., & Knaff, J. A. (2022). A Simple Model for Predicting the Tropical Cyclone Radius of Maximum Wind from Outer Size. (EOR). *Weather Forecasting*.

Chavas, D. R., Lin, N., & Emanuel, K. A. (2015). A Complete Tropical Cyclone Radial Wind Structure Model. Part I: Comparison with Observed Structure. *J. Atmos. Sci.*, *72(9)*, 3647-3662.

Chen, J., & Chavas, D. R. (2023). A Model for the Tropical Cyclone Wind Field Response to Idealized Landfall. *J. Atmos. Sci.*, *80*, 1163–1176.

Chen, J., Lin, S. J., Magnusson, L., Bender, M. A., Chen, X., Zhou, L. J., . . . Harris, L. (2019). Advancements in Hurricane Prediction with NOAA's Next Generation Forecast System. *Geophysical Research Letters*, *46(8)*.

Emanuel, K. A. (2004). Atmospheric Turbulence and Mesoscale Meteorology. In *Tropical cyclone energetics and structure* (p. 165–192). Cambridge University Press.

Emanuel, K. A., & Rotunno, R. (2011). Self-stratification of Tropical Cyclone Outflow. Part I: Implications for Storm Structure. *J. Atmos. Sci.*, *68*, 2236–2249.

Evans, J. L., & Hart, R. E. (2003). Objective Indicators of the Life Cycle Evolution of Extratropical Transition for Atlantic Tropical Cyclones. *Mon. Wea. Rev.*, *131(5)*, 909–925.

Feng, K., Ouyang, M., & Lin, N. (2022). Tropical Cyclone-blackout-heatwave Compound Hazard Resilience in a Changing Climate. *Nat Commun*, *13*, 4421.

Gao, K., Harris, L., Zhou, L., Bender, M., & Morin, M. (2021). On the Sensitivity of Hurricane Intensity and Structure to Horizontal Tracer Advection Schemes in FV3. *J. Atmos. Sci.*, *78*, 3007–3021.

Gori, A., & Lin, N. (2022). Projecting Compound Flood Hazard Under Climate Change with Physical Models and Joint Probability Methods. *Earth's Future.*.

Harris, L., Chen, X., Putman, W., Zhou, L., & Chen, J. H. (2021). A Scientific Description of the GFDL Finite-Volume Cubed-Sphere Dynamical Core. *NOAA technical memorandum OAR GFDL*, *2021-001*.

Harris, L., Zhou, L., Lin, S.-J., Chen, J.-H., X.Chen, Gao, K., & et al. (2020). GFDL SHiELD: A Unified System for Weather-to-Seasonal Prediction. *Journal of Advances in Modeling Earth Systems*, *12*, e2020MS002223.

Hersbach, H. (2010). Sea-surface Roughness and Drag Coefficient as Function of Neutral Wind Speed. *Internal Report from European Centre for Medium-Range Weather Forecasts (ECMWF)*. Retrieved from `https://www.ecmwf.int/node/9875`

Klotzbach, P. J., Chavas, D. R., Bell, M., Bowen, S., Gibney, E., & III, C. S. (2022). Characterizing Continental US Hurricane Risk: Which Intensity Metric is Best? *Journal of Geophysical Research: Atmospheres*, 127.

Knapp, K. R., Kruk, M. C., Levinson, D. H., Diamond, H. J., & Neumann, C. J. (2010). The International Best Track Archive for Climate Stewardship (IBTrACS): Unifying tropical cyclone best track data. *Bull. Amer. Meteor. Soc.*, *91*, 363-376.

Knutson, T., & Coauthors. (2020). Tropical Cyclones and Climate Change Assessment: Part II: Projected Response to Anthropogenic Warming. *Bull. Amer. Meteor. Soc.*, *101*, E303–E322.

Kossin, J. (2018). A Global Slowdown of Tropical-cyclone Translation Speed. *Nature*, *558*, 104-107.

Kossin, J. (2019). Reply to: Moon, I.-J. et al.; Lanzante, J. R. *Nature*, *570*, E16–E22.

Kossin, J., Emanuel, K. A., & Vecchi, G. A. (2014). The Poleward Migration of the Location of Tropical Cyclone Maximum Intensity. *Nature*, *509*, 349–352.

Landsea, C. W. (2007). Counting Atlantic Tropical Cyclones Back to 1900. *EOS Transactions American Geophysical Union*, *88(18)*.

Landsea, C. W., & Frankin, J. (2013). Atlantic Hurricane Database Uncertainty and Presentation of a new Database Format. *Monthly Weather Review*, *141(10)*, 3576–3592.

Li, L., & Chakraborty, P. (2020). Slower Decay of Landfalling Hurricanes in a Warming World. *Nature*, *587*, 230–234.

Lin, J., Emanuel, K., & K.Vigh, J. (2020). Forecasts of Hurricanes Using Large-Ensemble Outputs. *Weather and Forecasting*, *35(5)*, 1713-1731.

Masters, F. J., Vickery, P. J., Bacon, P., & Rappaport, E. N. (2010). Toward Objective, Standardized Intensity Estimates from Surface Wind Speed Observations. *Bull. Amer. Meteor. Soc.*, *91*, 1665–1681.

Mendelsohn, R., Emanuel, K., Chonabayashi, S., & Bakkensen, L. (2012). The Impact of Climate Change on Global Tropical Storm Damages. *Nat. Clim. Change*, *2*, 205-9.

Nolan, D. S., McNoldy, B., & Yunge, J. (2021). Evaluation of the Surface Wind Field over Land in WRF Simulations of Hurricane Wilma (2005). Part I: Model Initialization and Simulation Validation. *Mon. Wea. Rev.*, *149(3)*, 679-695.

Rappaport, E. (2014). Fatalities in the United States from Atlantic Tropical Cyclones:New Data and Interpretation. *Bull. Amer. Meteor. Soc.*, *95*, 341–346.

Smith, J., Baeck, M., Su, Y., Liu, M., & Vecchi, G. (2023). Strange Storms: Rainfall Extremes from the Remnants of Hurricane Ida (2021) in the Northeastern US. *Water Resources Research*, *59*, e2022WR033934.

Villarini, G., Goska, R., Smith, J. A., & Vecchi, G. A. (2014). North Atlantic Tropical Cyclones and U.S. Flooding. *Bull. Amer. Meteor. Soc.*, *95*, 1381–1388.

Wang, S., Lin, N., & Gori, A. (2022). Investigation of Tropical Cyclone Wind Models with Application to Storm Tide Simulations. *Journal of Geophysical Research: Atmospheres*.

Xi, D., Lin, N., & Smith, J. (2020). Evaluation of a Physics-Based Tropical Cyclone Rainfall Model for Risk Assessment. *Journal of Hydrometeorology*, *21(9)*, 2197-2218.

Zhai, A. R., & Jiang, J. H. (2014). Dependence of US Hurricane Economic Loss on Maximum Wind Speed and Storm Size. *Environ. Res. Lett.*, *9*, 064019.

Zhou, L. J., Lin, S. J., Chen, J. H., ad X. Chen, L. H., & Rees, S. L. (2019). Toward Convective-Scale Prediction within the Next Generation Global Prediction System. *Bulletin of the American Meteorological Society*, *100(7)*.

Zhu, Y. J., & Collins, J. M. (2021). Recent Rebounding of the Post-landfall Hurricane Wind Decay Period over the Continental United States. *Geophys Res Lett*, *70*, e2020GL092072.